

1 **Title**

2 Cognitive relevance of an evolutionarily new and variable prefrontal structure

3

4 **Authors and affiliations**

5 Ethan H. Willbrand^{1,2}, Samantha Jackson², Szeshuen Chen¹, Catherine B. Hathaway³, Willa I.

6 Voorhies¹, Silvia A. Bunge^{1,2*}, Kevin S. Weiner^{1,2*}

7

8 ¹*Department of Psychology, University of California, Berkeley, Berkeley, CA, 94720 USA*

9 ²*Helen Wills Neuroscience Institute, University of California, Berkeley, Berkeley, CA, 94720 USA*

10 ³*Cognitive Science, University of California, Berkeley, Berkeley, CA 94720 USA*

11 **Co-senior authors*

12

13 **Corresponding author:** Kevin S. Weiner

14 **Email:** kweiner@berkeley.edu

15

16 **Keywords:** neuroanatomy, MRI, sulcal morphology, reasoning, comparative biology, lateral

17 prefrontal cortex

18

19

20

21

22

23

24

25 **Abstract**

26 Identifying structural-functional correspondences is a major goal among biologists. In
27 neurobiology, recent findings identify relationships between performance on cognitive tasks and
28 the presence or absence of small, shallow indentations, or sulci, of the human brain. Here, we
29 tested if the presence or absence of one such sulcus, the paraintermediate frontal sulcus (pimfs-
30 v) in lateral prefrontal cortex, was related to relational reasoning in young adults from the Human
31 Connectome Project (ages 22-36). After manually identifying 2,877 sulci across 144 hemispheres,
32 our results indicate that the presence of the pimfs-v in the left hemisphere was associated with a
33 21-34% higher performance on a relational reasoning task. These findings have direct
34 developmental and evolutionary relevance as recent work shows that the presence or absence
35 of the pimfs-v is also related to reasoning performance in a pediatric cohort, and that the pimfs-v
36 is exceedingly rare in chimpanzees. Thus, the pimfs-v is a novel developmental, cognitive, and
37 evolutionarily relevant feature that should be considered in future studies examining how the
38 complex relationships among multiscale anatomical and functional features of the brain give rise
39 to abstract thought.

40 **Introduction**

41 Identifying structural-functional correspondences is a major goal across subdisciplines in
42 the biological sciences. In neurobiology and cognitive neuroscience, there is broad interest in
43 uncovering relationships between neuroanatomical features of the human brain and cognition —
44 especially for structures in parts of the brain that are largely human-specific. Given that 60-70%
45 of the human cerebral cortex is buried in indentations, or sulci [1–3], there continues to be great
46 interest in the relationships among sulcal morphology, functional representations, and cognition.
47 Previous work exploring this relationship has largely focused on the consistent and prominent
48 sulci within primary sensory cortices, such as the central and calcarine sulci [4–11]. Nevertheless,
49 recent work has begun to explore the less consistent and more variable sulci, such as small and
50 shallow sulci in association cortices that are not always present in a given hemisphere. For
51 example, recent studies have identified relationships between the presence or absence of specific
52 sulci in association cortices and individual differences in human cognitive abilities and clinical
53 conditions (for review see [12]), which could be mediated by differences in white matter
54 architecture in relation to these sulcal features [3,13–15].

55 To date, relationships between the presence/absence of variable sulci and cognition have
56 been most widely explored in the anterior cingulate cortex (ACC) [12]; here, we focus on variations
57 in the folding of the lateral prefrontal cortex (LPFC), a highly expanded region crucial for higher-
58 level functions such as abstract reasoning [16–22]. A combination of previous findings [23–25]
59 further motivated the present study, showing that a sulcus in anterior LPFC (ventral para-
60 intermediate frontal sulcus, pimfs-v) was variably present in children and adolescents [23,24] and
61 markedly rare in chimpanzees [25]. Further, the presence of left hemisphere pimfs-v in a sample
62 of 6-18-year-olds was associated with higher reasoning scores [24]. Building on these previous
63 results in the present study, we show that the sulcal patterning of the pimfs and the relationship
64 between the presence/absence of the pimfs-v and reasoning is a reliable and enduring individual

65 difference generalizing to an adult sample (ages 22-36). The reliable brain-behavior relationship
66 between the presence of the left pimfs-v and reasoning across age groups and studies is
67 important given a timely discussion among researchers regarding the reliability of brain-behavior
68 relationships [26–28]. We discuss these findings in the context of (i) the role of anterior LPFC and
69 reasoning across age groups and (ii) hypothesized relationships among the presence/absence of
70 sulci, the morphology of sulci, white matter architecture, and the efficiency of network communication
71 contributing to performance on cognitive tasks.

72

73 **Materials and Methods**

74 **(a) Participants**

75 Data for the young adult human cohort analyzed in the present study were taken from the Human
76 Connectome Project (HCP) database ([https://www.humanconnectome.org/study/hcp-young-](https://www.humanconnectome.org/study/hcp-young-adult/overview)
77 [adult/overview](https://www.humanconnectome.org/study/hcp-young-adult/overview)). Here we used 72 participants (50% female, aged between 22 and 36 years old).
78 These participants have also been used in our previous work [29,30].

79

80 **(b) Imaging data acquisition**

81 Anatomical T1-weighted (T1-w) MRI scans (0.7 mm voxel resolution) were obtained in native
82 space from the HCP database. First, the images obtained from the scans were averaged. Then,
83 reconstructions of the cortical surfaces of each participant were generated using FreeSurfer, a
84 software used for processing and analyzing human brain MRI images (v6.0.0,
85 surfer.nmr.mgh.harvard.edu). All subsequent sulcal labeling and extraction of anatomical metrics
86 were calculated from the cortical surface reconstructions of individual participants generated
87 through the HCP's custom-modified version of the FreeSurfer pipeline [31–33].

88

89 **(c) Behavioral data**

90 **(i) Overview**

91 In addition to structural and functional neuroimaging data, the Human Connectome project also
92 collected a wide range of behavioral metrics (motor, cognitive, sensory, and emotional processes)
93 from the NIH toolbox [34] that illustrate a set of core functions relevant to understanding the
94 relationships between human behavior and the brain (for task details see:
95 [https://wiki.humanconnectome.org/display/PublicData/HCP-YA+Data+Dictionary-
96 +Updated+for+the+1200+Subject+Release#HCPYADictionaryUpdatedforthe1200SubjectR
97 elease-Instrument](https://wiki.humanconnectome.org/display/PublicData/HCP-YA+Data+Dictionary-+Updated+for+the+1200+Subject+Release#HCPYADictionaryUpdatedforthe1200SubjectRelease-Instrument)). 71 of 72 participants in the present project had behavioral scores. Below we
98 describe the three behavioral tests used.

99

100 **(ii) Reasoning task**

101 The ability to reason about the patterns, or relations, among disparate pieces of information has
102 long been recognized as central to human reasoning and learning (e.g., [35–37]). Tests of
103 relational reasoning assess the ability to integrate and generalize across multiple pieces of
104 information; as a result, they help to predict real-world performance in a variety of domains [38].
105 Here, we used the behavioral data obtained for each participant measuring reasoning skills using
106 a measure of relational reasoning, the Penn Progressive Matrices Test from the NIH toolbox [34].
107 This test is highly similar to the classic Raven’s Progressive Matrices [39], WISC-IV Matrix
108 Reasoning task [40], and other task variants that are ubiquitous in assessments of so-called “fluid
109 intelligence.” Participants must consider how shapes in a stimulus array — a 2x2, 3x3, or 1x5
110 arrangement of squares, in the case of the current task — are related to one another (e.g., an
111 increase, across a row or column, in the number of lines superimposed on a shape) [41–46].
112 Specifically, participants must extrapolate from the visuospatial relations present in the array and
113 select among five options the shape that completes the matrix. The task is composed of 24
114 different matrices to complete, in order of increasing difficulty. Testing is discontinued after five
115 incorrect choices in a row, and the total score is calculated.

116

117 **(iii) *Processing speed task***

118 To measure processing speed, participants completed the Pattern Comparison Processing
119 Speed Test from the same NIH toolbox [34]. This test has been designed to measure the speed
120 of cognitive processing based on the participant's ability to discern as quickly as possible whether
121 two adjacent pictures are identical. In this test, participants must consider several possible
122 differences (addition/removal of an element or the color or number of elements on the pictures).
123 They indicate via a yes-no button press whether the two stimuli are identical, and their final score
124 corresponds to the number of trials answered correctly during a 90-second period.

125

126 **(iv) *Working memory task***

127 To measure working memory performance, participants completed the List Sorting Working
128 Memory Test from the NIH toolbox [34]. In this task, each participant sequences different visually
129 and orally presented stimuli (alongside a sound clip and written text for the name of the item) in
130 two conditions: 1-List and 2-List. In the former, participants order a series of objects (food or
131 animals) from smallest to largest. In the latter, participants are presented with both object groups
132 (food and animals) and must report the food in size order and then the animals in size
133 order. Crucially, completing this task not only requires working memory manipulation and
134 maintenance but also relational thinking, given that it also requires participants to assess the
135 relationship between the different stimuli. To report the items in size order it is necessary to
136 compare pairs of stimuli and then engage in transitive inference across pairs (e.g., as reported by
137 [47,48]).

138

139 **(d) Morphological analyses**

140 **(i) *Cortical surface reconstruction***

141 FreeSurfer's automated segmentation tools [31,32,49] were used to generate cortical surface
142 reconstructions. Briefly, each anatomical T1-w image was segmented to separate gray from white
143 matter, and the resulting boundary was used to reconstruct the cortical surface for each
144 participant [31,50]. Each reconstruction was visually inspected for segmentation errors, and these
145 were manually corrected when necessary.

146 Cortical surface reconstructions facilitate the identification of shallow tertiary sulci
147 compared to post-mortem tissue – for two main reasons. First, T1-w MRI protocols are not ideal
148 for imaging vasculature; thus, the vessels that typically obscure the tertiary sulcal patterning in
149 post-mortem brains are not imaged on standard-resolution T1-w MRI scans [30,51]. Indeed,
150 indentations produced by these smaller vessels that obscure the tertiary sulcal patterning are
151 visible in freely available datasets acquired at high field (7T) and micron resolution (100–250 μm)
152 [52,53]. Thus, the present resolution of our T1s (0.7 mm isotropic) is sufficient to detect the
153 shallow indentations of tertiary sulci yet is not confounded by smaller indentations produced by
154 the vasculature. Second, cortical surface reconstructions are created from the boundary between
155 gray and white matter; unlike the outer surface, this inner surface is not obstructed by blood
156 vessels [51,54].

157

158 **(ii) Defining the presence and prominence of the para-intermediate middle frontal sulcus**

159 Individuals typically have anywhere from three to five tertiary sulci within the middle frontal gyrus
160 (MFG) in LPFC [23,30,55,56]. The posterior MFG contains three of these sulci, which are present
161 in all participants: the anterior (pmfs-a), intermediate (pmfs-i), and posterior (pmfs-p) components
162 of the posterior middle frontal sulcus (pmfs). In contrast, the tertiary sulcus within the anterior
163 MFG, the para-intermediate middle frontal sulcus (pimfs), is variably present. A given hemisphere
164 can have zero, one, or two pimfs components (examples in **figure 1**). As described in prior work
165 [24,57,58], the dorsal and ventral components of the pimfs (pimfs-d and pimfs-v) were generally
166 defined using the following two-fold criterion: i) the sulci ventrolateral to the horizontal and ventral

167 components of the intermediate middle frontal sulcus, respectively, and ii) superior and/or anterior
168 to the mid-anterior portion of the inferior frontal sulcus.

169 We first manually defined the pimfs within each individual hemisphere with *tksurfer* [30].
170 Manual lines were drawn on the *inflated* cortical surface to define sulci based on the most recent
171 schematics of pimfs and sulcal patterning in LPFC by Petrides [57], as well as by the *pial* and
172 *smoothwm* surfaces of each individual [30]. In some cases, the precise start or end point of a
173 sulcus can be difficult to determine on a surface [59]. Thus, using the *inflated*, *pial*, and *smoothwm*
174 surfaces to inform our labeling allowed us to form a consensus across surfaces and clearly
175 determine each sulcal boundary. For each hemisphere, the location of the pimfs was confirmed
176 by three trained independent raters (E.H.W., S.M., S.C.) and finalized by a neuroanatomist
177 (K.S.W.). Although this project focused on a single sulcus, the manual identification of all LPFC
178 sulci (2,877 sulcal definitions across all 72 participants) was required to ensure the most accurate
179 definitions of the pimfs components. For in-depth descriptions of all LPFC sulci, see [23,30,55–
180 57,60]. The incidence rates of the two pimfs components (i.e., sulcal patterning) were compared
181 within and between hemispheres with Chi-squared and Fischer exact tests, respectively. Chi-
182 squared tests were carried out with the `chisq.test` function from the stats R package [all statistical
183 tests were implemented in R (v4.0.1; <https://www.r-project.org/>)]. Fisher's exact tests were carried
184 out with the `fisher.test` function from the stats R package.

185

186 **(e) Behavioral analyses: Relating the presence of the pimfs to reasoning performance**

187 Participant age and gender were not considered in these analyses, as they were not associated
188 with reasoning performance (*age*: $r = -0.04$, $p = 0.75$; *gender*: $t = 1.01$, $p = 0.32$). We first ran two-
189 sample t-tests to assess whether the number of components in each hemisphere (*two* vs *less*
190 *than two*) related to reasoning performance (Penn Progressive Matrices Test). Next, to determine
191 if the presence of a specific pimfs component was related to reasoning performance, we ran
192 additional two-sample t-tests to test for an effect of presence of the pimfs-v and pimfs-d (*present*

193 vs *absent*) in each hemisphere. As presented below, this model revealed that the presence of left
194 pimfs-v was linked to reasoning performance. To determine whether this result was impacted by
195 differences in sample size between participants with and without this sulcus, we iteratively
196 sampled a subset of participants from the left pimfs-v present group (N = 57) to match that of the
197 left pimfs-v absent group (N = 14) 1000 times and conducted a Welch's t-test for each sampling
198 (to account for the distributions potentially being unequal when resampling). To evaluate the
199 results, we report the median and 95% confidence interval for the effect size.

200 To ascertain whether the observed relationship between sulcal morphology and cognition
201 is specific to reasoning performance, or generalizable to other measures of cognitive processing,
202 we tested this sulcal-behavior relationship with measures of processing speed (Pattern
203 Comparison Processing Speed Test) and working memory (List Sorting Working Memory Test).
204 Participant age and gender were not considered in these analyses, as they were not reliably
205 associated with processing speed (*age*: $r = -0.21$, $p = 0.08$; *gender*: $t = 0.06$, $p = 0.95$) or working
206 memory (*age*: $r = -0.03$, $p = 0.81$; *gender*: $t = 1.59$, $p = 0.12$). Two-sample t-tests were run to
207 assess for differences in performance on each measure based on left pimfs-v presence (*present*
208 vs *absent*). If either test showed a strong association, we then used the Akaike Information
209 Criterion (AIC) to compare the model predictions to reasoning predictions. Briefly, the AIC
210 provides an estimate of in-sample prediction error and is suitable for non-nested model
211 comparison. By comparing AIC scores, we are able to assess the relative performance of the two
212 models. If the ΔAIC is >2 , it suggests an interpretable difference between models. If the ΔAIC is
213 >10 , it suggests a strong difference between models, with the lower AIC value indicating the
214 preferred model [61,62].

215 T-tests were implemented with the `t.test` function from the R stats package. T-test effect
216 sizes are reported with the Cohen's d (d) metric. The median and 95% confidence intervals were
217 calculated with the `MedianCI` function from the `DescTools` R package. AIC values were quantified
218 with the `AIC` function from the stats R package.

219

220 **(f) Probability maps**

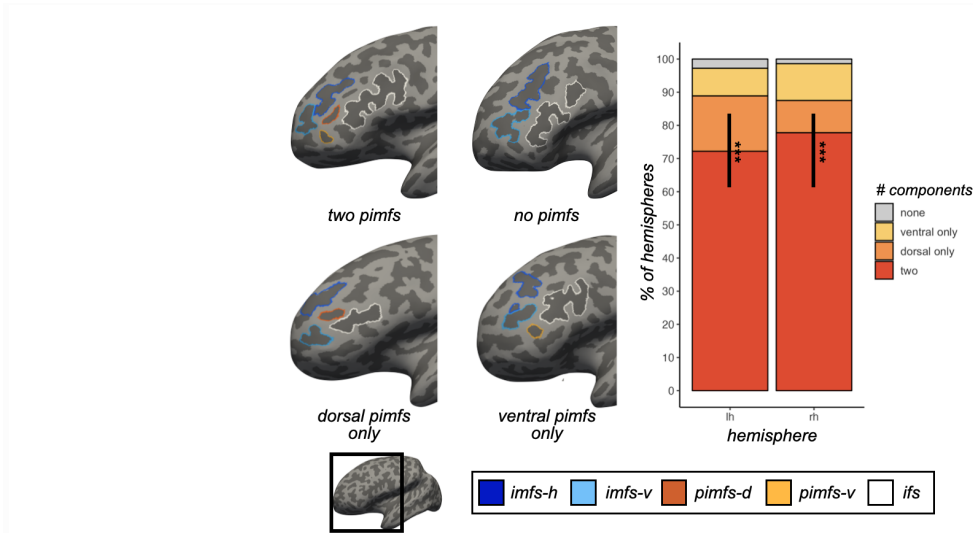
221 As in prior work [23,25,29,30,63], sulcal probability maps were calculated to display the vertices
222 with the highest alignment across participants for a given sulcus. To generate these maps, the
223 label file for each pimfs component was transformed from the individual to the fsaverage surface.
224 Once transformed into this common template space, we calculated, for each vertex, the proportion
225 of participants for whom the vertex is labeled as the given pimfs component. For vertices where
226 the pimfs components overlapped, we employed a greedy, "winner-take-all" approach such that
227 the component with the highest overlap across participants was assigned to a given vertex. In
228 addition to providing unthresholded maps, we also constrain these maps to maximum probability
229 maps (MPMs) at 10% and 20% participant overlap to increase interpretability (10% overlap MPMs
230 are shown in **figure 3**).

231

232 **Results**

233 Anatomical and behavioral data were randomly selected from 72 participants (50%
234 female, aged 22-36) from the HCP study [64]. Cortical reconstructions were then generated from
235 T1-weighted MRI scans using FreeSurfer [31,32,49]. Following previously established criteria and
236 the definition of 2,877 sulci across 144 hemispheres (**Materials and Methods**), we manually
237 defined the component(s) of the pimfs, when present. Four example hemispheres are presented
238 in **figure 1**. Analyses on the patterning of the pimfs found that it was more common for young
239 adults to have two components in a given hemisphere (*left*: 72.22% of participants; *right*: 77.78%)
240 than either one (*left*: 25%; *right*: 20.83%) or none (*left*: 2.78%; *right*: 1.39%; $\chi^2 > 54$, $p < 1.50e-12$

241 in both hemispheres). There was no hemispheric asymmetry in incidence rates ($p = 0.66$; **figure**
242 **1**), and when only one pimfs component was present, it was equally likely to be a dorsal or ventral
243 component ($\chi^2 < 2$, $p > .15$ in both hemispheres; **figure 1**). These incidence rates were similar to
244 those observed in children and adolescents [24], which was anticipated given that sulci are formed
245 during gestation [3,12,55,65,66].

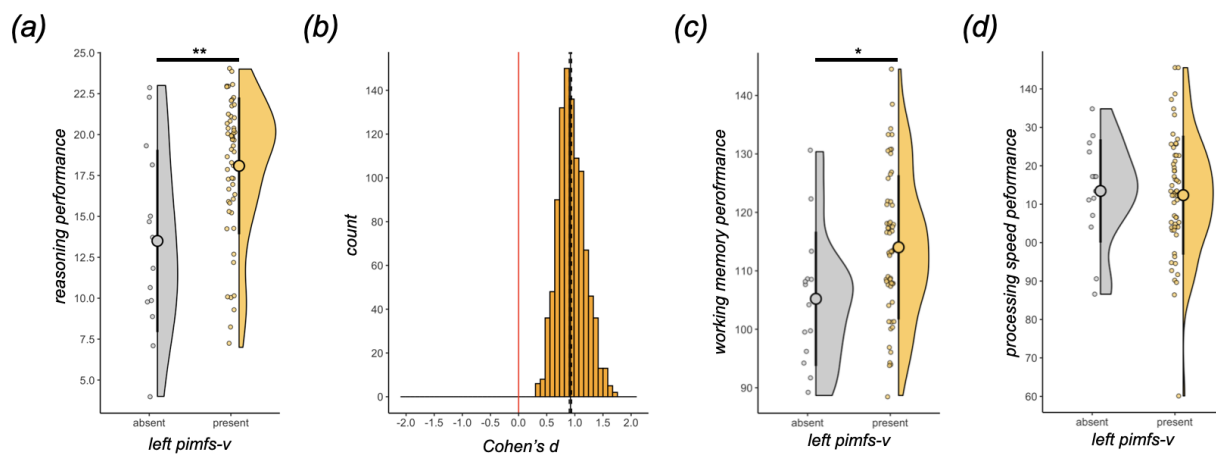


246

247 **Figure 1. The incidence of the pimfs is highly variable across individuals and hemispheres.**
248 *Left:* Inflated left hemispheres (sulci: dark gray; gyri: light gray; cortical surfaces are not to scale)
249 depicting the four types of the para-intermediate frontal sulcus (pimfs): (i) both components
250 present, (ii) neither present, (iii) dorsal component present, (iv) ventral component present. The
251 prominent sulci bounding the pimfs are also shown: the horizontal (imfs-h) and ventral (imfs-v)
252 intermediate frontal sulci and inferior frontal sulcus (ifs). Each sulcus is colored according to the
253 bottom legend. *Right:* Stacked bar plot depicting the incidence of the pimfs components in both
254 the left (lh) and right (rh) hemispheres across the sample of 72 young adults. Each type of the
255 pimfs is colored according to the rightward legend. (***, $p < .001$)
256

257 As the pimfs is variably present among young adults, we statistically tested whether this
258 variability was related to reasoning performance, as previously found for children and adolescents
259 [24]. Reasoning performance was quantified as scores on the Penn Progressive Matrices Test
260 from the NIH Toolbox [34], a relational reasoning task similar to the WISC-IV Matrix Reasoning
261 task used previously [23,24,40]. The presence of two pimfs components in the left hemisphere
262 was associated with 21% better reasoning performance relative to either one or none ($t(69) =$
263 2.54 , $p = 0.01$, $d = 0.67$). We had found previously in children and adolescents that this effect was

264 driven by the presence or absence of the left hemisphere pimfs-v [24]. Here, we find that this is
265 also true in young adults. The presence of left pimfs-v was associated with 34% higher reasoning
266 scores ($t(69) = 3.44$, $p = 0.001$, $d = 1.03$; **figure 2a**); no other pimfs component in either
267 hemisphere showed this effect ($t_s < 1.32$, $p_s > 0.19$, $d_s < 0.47$). To account for the difference in
268 sample sizes between adults with and without the left pimfs-v, we iteratively sampled a size-
269 matched subset of the left pimfs-v present group 1000 times. This procedure confirmed the
270 behavioral difference (median, 95% CI $d = 0.92$, $0.90-0.94$; **figure 2b**).



271

272 **Figure 2. The presence of the para-intermediate frontal sulcus is related to relational**
273 **thinking.** (a) Raincloud plots [67] depicting Penn Progressive Matrices task score as a function
274 of left pimfs-v presence in young adults (present, $N = 57$; absent, $N = 14$). The large dots and
275 error bars represent the mean \pm std reasoning score, and the violin plots show the kernel density
276 estimate. The smaller dots indicate individual participants. (b) Histogram visualizing the results of
277 the iterative resampling of the left pimfs-v present group in (A) 1000 times. The distribution of the
278 effect size (Cohen's d) is shown, along with the median (black line) and 95% CI (dotted lines).
279 The red line corresponds to zero to emphasize that none of the comparisons ever showed a
280 reverse relationship in reasoning scores (i.e., left pimfs-v absent having higher reasoning scores
281 than left pimfs-v present). (c) Same format as (a) for the List Sorting task. (d) Same format as (a)
282 for the Pattern Completion task. (**, $p < .01$; *, $p < .05$)
283

284 Finally, to assess the generalizability and/or specificity of this brain-behavior relationship,
285 we tested whether the presence of left pimfs-v was associated with performance on tests of
286 working memory (WM; List Sorting Working Memory Test) and/or processing speed (Pattern
287 Comparison Processing Speed Test), foundational cognitive skills that support reasoning [68–

288 72]. As noted above, the WM test administered to HCP participants involves reordering items
289 according to their relative size, thereby placing demands on relational thinking (**Materials and**
290 **Methods**). Left pimfs-v presence was positively associated with 9% better performance on the
291 WM test ($t(69) = 2.42$, $p = 0.01$, $d = 0.72$; **figure 2c**). While this effect was significant, it was not
292 as large as that observed for the reasoning test ($\Delta AIC_{(\text{working memory} - \text{reasoning})} = 142.23$). By contrast,
293 left pimfs-v presence was not related to processing speed test performance ($t(69) = -0.24$, $p =$
294 0.81 , $d = -0.07$; **figure 2d**), a finding suggesting some degree of specificity in this brain–behavior
295 relation and consistent with previous anatomical-cognitive findings in our pediatric cohort [23,24].
296

297 **Discussion**

298 Integrating these data with prior work, at least one pimfs component is identifiable in the
299 majority of human hemispheres [277/288 (96%)], with comparable incidence between young
300 adults [141/144 (97%)] and children and adolescents [136/144 (94%)] [24]. However, these
301 incidence rates are in stark contrast to what is observed in chimpanzees [2/60 (3%; one
302 chimpanzee)] [25], emphasizing that the pimfs is a largely human-specific cortical structure.
303 Further, this structure exhibits prominent variability in humans that is robustly linked to variability
304 in reasoning performance, both in young adulthood (ages 22-36), as reported here, and in
305 childhood and adolescence (ages 6-18) [24]. Considering that smaller, shallower (tertiary) sulci in
306 association cortices, such as the pimfs, develop later in gestation than larger, deeper sulci like
307 the central and calcarine sulci [65,66,73], a testable evolutionary and developmental hypothesis
308 is that the higher incidence of the pimfs in humans — and cortical sulci in general [25,29,57,74]
309 — is a consequence of the markedly protracted and greater intrauterine brain growth generally
310 seen in humans compared to chimpanzees [75].

311 With regard to the relationship to reasoning performance, it is notable that the pimfs-v
312 appears to co-localize with rostrolateral PFC (RLPFC), a functionally defined region consistently

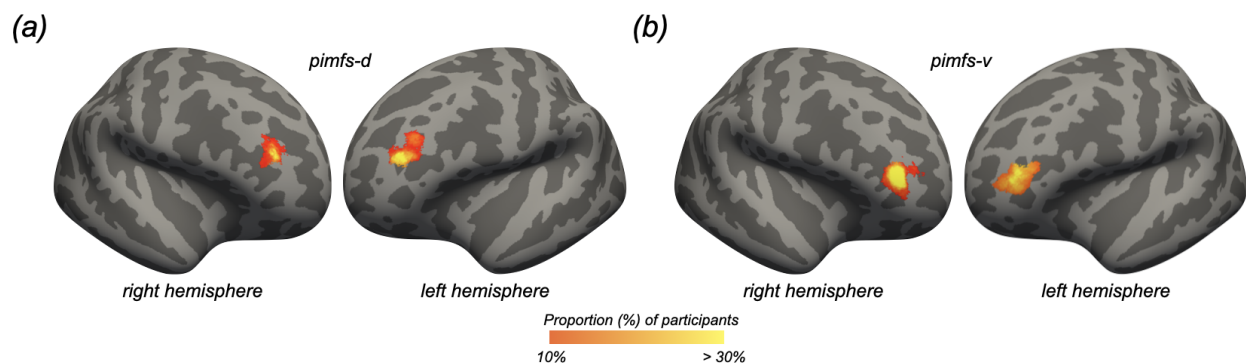
313 implicated in a variety of reasoning tasks by both neuropsychological and fMRI studies [19,72,76–
314 81], including matrix reasoning tasks like the one used in the present study [42,82,83]. Tightly
315 controlled fMRI studies have also pointed to the left RLPFC as playing a particularly strong role
316 in relational thinking [72,84]. However, precise localization of RLPFC at the individual level has
317 been impeded by normalization and group averaging of fMRI activation. As such, future work
318 should assess whether the pimfs-v is a useful landmark that predicts the location of functionally
319 defined RLPFC in individual participants, given that other sulci in association cortices have been
320 identified as functional landmarks [29,85–89].

321 The extensive variability in the presence/absence of the pimfs components across
322 individuals, and the rarity of the pimfs in chimpanzees, likely also reflects differences in white
323 matter architecture. For example, RLPFC is disproportionately expanded in humans relative to
324 non-human primates, which has been hypothesized to contribute to species differences in
325 reasoning capacity [77,90]. Further, the presence/absence and morphology of sulci are theorized
326 to be anatomically linked to cortical white matter [12,14,30,91–93]. Given that the pimfs is rare in
327 chimpanzees [25], the presence of left pimfs-v could reflect evolutionarily expanded white matter
328 properties that enhance neural communication in this higher cognitive area [3,13–15]. Tentatively
329 supporting this idea, the white matter properties and functional connectivity of long-range
330 connections involving RLPFC have been linked to reasoning performance and developmental
331 growth [94]. Future research should investigate this multiscale, mechanistic relationship
332 describing the neural correlates of reasoning, integrating structural, functional, and behavioral
333 data.

334 In this young adult sample, we showed that the presence of left pimfs-v was associated
335 not only with 34% (on average) better performance on a test of relational reasoning, but also 9%
336 (on average) better performance on a test of WM that requires relational thinking. On the other
337 hand, this sulcal feature was unrelated to processing speed. In our pediatric sample, the presence
338 of left pimfs-v was not related either to processing speed or to WM. In that prior study, the test of

339 WM was a standard measure that involves repeating a series of digits in either the forward or
340 reverse order (WISC-IV Digit Span task) [40]. Given that participants in the two samples
341 completed different WM tasks, it is an open question whether presence/absence of the pimfs-v is
342 only linked to WM when the task requires relational thinking — a plausible hypothesis, given that
343 RLPFC is not thought to be centrally involved in WM per se (e.g., [47,48]). Future research should
344 further explore the specificity of the cognitive effects of presence/absence of the left pimfs-v, as
345 well as test whether and how the presence/absence of the right pimfs-v and left/right pimfs-d are
346 cognitively relevant in other domains.

347 To date, the patterning and cognitive relevance of the pimfs has only been examined in
348 neurotypical populations [23,24,56]. Numerous studies of disorders such as schizophrenia,
349 autism spectrum disorder, obsessive-compulsive disorder, and fronto-temporal dementia have
350 found that variations in sulcal incidence are clinically relevant — although most of this work has
351 focused on the ACC (e.g., [95–103]) and orbitofrontal cortex (for review see [104]). Thus, the
352 present results raise the question of whether the incidence of the pimfs differs in any of the clinical
353 populations that exhibit impaired reasoning. Schizophrenia is a prime candidate for future
354 investigations, given that it is marked by impaired reasoning [105–110] and has repeatedly been
355 associated with altered RLPFC structure and function [111–117]. To help guide future studies
356 examining the cognitive, evolutionary, developmental, clinical, and functional relevance of the
357 pimfs, we share probabilistic predictions of the pimfs from our data (**figure 3; Data accessibility**).



358

359 **Figure 3. Maximum probability maps for the para-intermediate frontal sulcus.** Maximum
360 probability maps (MPMs) for the pimfs-d (*a*) and pimfs-v (*b*) overlaid on the inflated fsaverage
361 cortical surface (sulci: dark gray; gyri: light gray; cortical surfaces are not to scale). To generate
362 the MPMs, each label was transformed from each individual to the fsaverage surface. For each
363 vertex, the proportion of participants for whom that vertex is labeled as the given sulcus (the
364 warmer the color, the higher the overlap) was calculated. In the cases in which the vertices for
365 each component overlapped, the sulcus with the highest overlap across participants was
366 assigned to that vertex. For visual clarity, the MPMs were thresholded to 10% overlap across
367 participants.
368

369 In conclusion, we have extended prior work in children and adolescents [24] by showing
370 that the presence of the left hemisphere pimfs-v is also cognitively relevant in young adulthood.
371 The combination of findings across studies empirically shows that the presence/absence of the
372 pimfs-v is a novel developmental, cognitive, and evolutionarily relevant feature that should be
373 considered in future studies in neurotypical and clinical populations examining how the complex
374 relationships among multiscale anatomical and functional features of the brain give rise to abstract
375 thought.

376

377

378

379

380

381

382 **Ethics statement**

383 HCP consortium data were previously acquired using protocols approved by the Washington
384 University Institutional Review Board.

385

386 **Competing interests statement**

387 The authors declare no competing financial interests.

388

389 **Data accessibility statement**

390 Data, analysis pipelines, and pimfs probability maps will be made freely available on GitHub upon
391 publication (https://github.com/cnl-berkeley/stable_projects/). Requests for further information or
392 raw data should be directed to the Corresponding Author, Kevin S. Weiner
393 (kweiner@berkeley.edu).

394

395 **Author contributions statement**

396 EHW, SAB, and KSW designed research; EHW, SJ, SC, CBH, WIV, and KSW performed manual
397 sulcal labeling; EHW, SAB, and KSW analyzed data; EHW, SAB, and KSW wrote the paper; all
398 authors gave final approval to the paper before submission.

399

400 **Funding information**

401 This research was supported by NICHD R21HD100858 (Weiner, Bunge), an NSF CAREER
402 Award 2042251 (Weiner), and an NSF-GRFP fellowship (Voorhies). Young adult neuroimaging
403 and behavioral data were provided by the HCP, WU-Minn Consortium (Principal Investigators:
404 David Van Essen and Kamil Ugurbil; NIH Grant 1U54-MH-091657) funded by the 16 NIH Institutes
405 and Centers that support the NIH Blueprint for Neuroscience Research, and the McDonnell
406 Center for Systems Neuroscience at Washington University.

407

408 **Acknowledgments**

409 We thank Jewelia Yao and Jacob Miller for their assistance defining other additional lateral
410 prefrontal cortex sulci across age groups. We also thank the HCP researchers for participant
411 recruitment and data collection and sharing, as well as the participants who took part in the study.

412

413 References

- 414 1. Van Essen DC. 2007 4.16 - Cerebral Cortical Folding Patterns in Primates: Why They Vary
415 and What They Signify. In *Evolution of Nervous Systems* (ed JH Kaas), pp. 267–276.
416 Oxford: Academic Press.
- 417 2. Zilles K, Armstrong E, Schleicher A, Kretschmann H-J. 1988 The human pattern of
418 gyrification in the cerebral cortex. *Anatomy and Embryology*. **179**, 173–179.
419 (doi:10.1007/bf00304699)
- 420 3. Zilles K, Palomero-Gallagher N, Amunts K. 2013 Development of cortical folding during
421 evolution and ontogeny. *Trends Neurosci*. **36**, 275–284.
- 422 4. Yousry TA, Schmid UD, Alkadhi H, Schmidt D, Peraud A, Buettner A, Winkler P. 1997
423 Localization of the motor hand area to a knob on the precentral gyrus. A new landmark.
424 *Brain* **120 (Pt 1)**, 141–157.
- 425 5. Boling W, Olivier A, Bittar RG, Reutens D. 1999 Localization of hand motor activation in
426 Broca's pli de passage moyen. *J. Neurosurg*. **91**, 903–910.
- 427 6. Hinds OP *et al.* 2008 Accurate prediction of V1 location from cortical folds in a surface
428 coordinate system. *Neuroimage* **39**, 1585–1599.
- 429 7. Cykowski MD, Coulon O, Kochunov PV, Amunts K, Lancaster JL, Laird AR, Glahn DC, Fox
430 PT. 2008 The central sulcus: an observer-independent characterization of sulcal landmarks
431 and depth asymmetry. *Cereb. Cortex* **18**, 1999–2009.
- 432 8. Li S *et al.* 2010 Mapping surface variability of the central sulcus in musicians. *Cereb. Cortex*
433 **20**, 25–33.
- 434 9. Wandell BA, Winawer J. 2011 Imaging retinotopic maps in the human brain. *Vision Res*. **51**,
435 718–737.
- 436 10. Benson NC, Butt OH, Datta R, Radoeva PD, Brainard DH, Aguirre GK. 2012 The
437 retinotopic organization of striate cortex is well predicted by surface topology. *Curr. Biol*. **22**,
438 2081–2085.
- 439 11. Sun ZY, Klöppel S, Rivière D, Perrot M, Frackowiak R, Siebner H, Mangin J-F. 2012 The
440 effect of handedness on the shape of the central sulcus. *Neuroimage* **60**, 332–339.
- 441 12. Cachia A, Borst G, Jardri R, Raznahan A, Murray GK, Mangin J-F, Plaze M. 2021 Towards
442 Deciphering the Fetal Foundation of Normal Cognition and Cognitive Symptoms From
443 Sulcation of the Cortex. *Front. Neuroanat*. **15**, 712862.
- 444 13. Van Essen DC. 1997 A tension-based theory of morphogenesis and compact wiring in the
445 central nervous system. *Nature* **385**, 313–318.
- 446 14. Van Essen DC. 2020 A 2020 view of tension-based cortical morphogenesis. *Proc. Natl.*
447 *Acad. Sci. U. S. A.* (doi:10.1073/pnas.2016830117)
- 448 15. White T, Su S, Schmidt M, Kao C-Y, Sapiro G. 2010 The development of gyrification in
449 childhood and adolescence. *Brain Cogn*. **72**, 36–45.

- 450 16. Luria AR. 1966 *Higher Cortical Functions in Man*. Springer US.
- 451 17. Milner B, Petrides M. 1984 Behavioural effects of frontal-lobe lesions in man. *Trends*
452 *Neurosci.* **7**, 403–407.
- 453 18. Stuss DT, Knight RT. 2013 *Principles of Frontal Lobe Function*. OUP USA.
- 454 19. Urbanski M *et al.* 2016 Reasoning by analogy requires the left frontal pole: lesion-deficit
455 mapping and clinical implications. *Brain* **139**, 1783–1799.
- 456 20. Donahue CJ, Glasser MF, Preuss TM, Rilling JK, Van Essen DC. 2018 Quantitative
457 assessment of prefrontal cortex in humans relative to nonhuman primates. *Proc. Natl.*
458 *Acad. Sci. U. S. A.* **115**, E5183–E5192.
- 459 21. Smaers JB, Gómez-Robles A, Parks AN, Sherwood CC. 2017 Exceptional Evolutionary
460 Expansion of Prefrontal Cortex in Great Apes and Humans. *Curr. Biol.* **27**, 714–720.
- 461 22. Smaers JB *et al.* 2021 The evolution of mammalian brain size. *Sci Adv* **7**.
462 (doi:10.1126/sciadv.abe2101)
- 463 23. Voorhies WI, Miller JA, Yao JK, Bunge SA, Weiner KS. 2021 Cognitive insights from tertiary
464 sulci in prefrontal cortex. *Nat. Commun.* **12**, 5122.
- 465 24. Willbrand EH, Voorhies WI, Yao JK, Weiner KS, Bunge SA. 2022 Presence or absence of a
466 prefrontal sulcus is linked to reasoning performance during child development. *Brain Struct.*
467 *Funct.* **227**, 2543–2551.
- 468 25. Hathaway CB, Voorhies WI, Sathishkumar N, Mittal C, Yao JK, Miller JA, Parker BJ,
469 Weiner KS. 2022 Defining tertiary sulci in lateral prefrontal cortex in chimpanzees using
470 human predictions. *bioRxiv.* , 2022.04.12.488091. (doi:10.1101/2022.04.12.488091)
- 471 26. Marek S *et al.* 2022 Reproducible brain-wide association studies require thousands of
472 individuals. *Nature* **603**, 654–660.
- 473 27. Gratton C, Nelson SM, Gordon EM. 2022 Brain-behavior correlations: Two paths toward
474 reliability. *Neuron.* **110**, 1446–1449.
- 475 28. Westlin C *et al.* 2023 Improving the study of brain-behavior relationships by revisiting basic
476 assumptions. *Trends Cogn. Sci.* (doi:10.1016/j.tics.2022.12.015)
- 477 29. Willbrand EH *et al.* 2022 Uncovering a tripartite landmark in posterior cingulate cortex.
478 *Science Advances* **8**, eabn9516.
- 479 30. Miller JA, Voorhies WI, Lurie DJ, D’Esposito M, Weiner KS. 2021 Overlooked Tertiary Sulci
480 Serve as a Meso-Scale Link between Microstructural and Functional Properties of Human
481 Lateral Prefrontal Cortex. *J. Neurosci.* **41**, 2229–2244.
- 482 31. Dale AM, Fischl B, Sereno MI. 1999 Cortical surface-based analysis. I. Segmentation and
483 surface reconstruction. *Neuroimage* **9**, 179–194.
- 484 32. Fischl B, Sereno MI, Dale AM. 1999 Cortical surface-based analysis. II: Inflation, flattening,
485 and a surface-based coordinate system. *Neuroimage* **9**, 195–207.

- 486 33. Glasser MF *et al.* 2013 The minimal preprocessing pipelines for the Human Connectome
487 Project. *Neuroimage* **80**, 105–124.
- 488 34. Barch DM *et al.* 2013 Function in the human connectome: task-fMRI and individual
489 differences in behavior. *Neuroimage* **80**, 169–189.
- 490 35. James W. 1890 The principles of psychology, Vol I. (doi:10.1037/10538-000)
- 491 36. James W. 1890 The Principles Of Psychology Volume II By William James (1890).
- 492 37. Cattell RB. 1943 The measurement of adult intelligence. *Psychol. Bull.* **40**, 153–193.
- 493 38. Alexander PA. 2016 Relational thinking and relational reasoning: harnessing the power of
494 patterning. *NPJ Sci Learn* **1**, 16004.
- 495 39. Raven JC. 1941 Standardization of progressive matrices, 1938. *Br. J. Med. Psychol.* **19**,
496 137–150.
- 497 40. Wechsler D. 1949 Wechsler Intelligence Scale for Children; manual. **113**.
- 498 41. Prabhakaran V, Smith JA, Desmond JE, Glover GH, Gabrieli JD. 1997 Neural substrates of
499 fluid reasoning: an fMRI study of neocortical activation during performance of the Raven's
500 Progressive Matrices Test. *Cogn. Psychol.* **33**, 43–63.
- 501 42. Christoff K, Prabhakaran V, Dorfman J, Zhao Z, Kroger JK, Holyoak KJ, Gabrieli JD. 2001
502 Rostrolateral prefrontal cortex involvement in relational integration during reasoning.
503 *Neuroimage* **14**, 1136–1149.
- 504 43. Conway ARA, Kane MJ, Bunting MF, Hambrick DZ, Wilhelm O, Engle RW. 2005 Working
505 memory span tasks: A methodological review and user's guide. *Psychon. Bull. Rev.* **12**,
506 769–786.
- 507 44. Gray JR, Chabris CF, Braver TS. 2003 Neural mechanisms of general fluid intelligence.
508 *Nat. Neurosci.* **6**, 316–322.
- 509 45. Gray JR, Burgess GC, Schaefer A, Yarkoni T, Larsen RJ, Braver TS. 2005 Affective
510 personality differences in neural processing efficiency confirmed using fMRI. *Cogn. Affect.*
511 *Behav. Neurosci.* **5**, 182–190.
- 512 46. Wendelken C, Nakhachenko D, Donohue SE, Carter CS, Bunge SA. 2008 'Brain is to
513 thought as stomach is to ??': investigating the role of rostralateral prefrontal cortex in
514 relational reasoning. *J. Cogn. Neurosci.* **20**, 682–693.
- 515 47. Wendelken C, Bunge SA, Carter CS. 2008 Maintaining structured information: an
516 investigation into functions of parietal and lateral prefrontal cortices. *Neuropsychologia* **46**,
517 665–678.
- 518 48. Wendelken C, Bunge SA. 2010 Transitive inference: distinct contributions of rostralateral
519 prefrontal cortex and the hippocampus. *J. Cogn. Neurosci.* **22**, 837–847.
- 520 49. Fischl B, Sereno MI, Tootell RB, Dale AM. 1999 High-resolution intersubject averaging and
521 a coordinate system for the cortical surface. *Hum. Brain Mapp.* **8**, 272–284.

- 522 50. Wandell BA, Chial S, Backus BT. 2000 Visualization and measurement of the cortical
523 surface. *J. Cogn. Neurosci.* **12**, 739–752.
- 524 51. Weiner KS, Natu VS, Grill-Spector K. 2018 On object selectivity and the anatomy of the
525 human fusiform gyrus. *Neuroimage* **173**, 604–609.
- 526 52. Edlow BL *et al.* 2019 7 Tesla MRI of the ex vivo human brain at 100 micron resolution. *Sci*
527 *Data* **6**, 244.
- 528 53. Lüsebrink F, Sciarra A, Mattern H, Yakupov R, Speck O. 2017 T1-weighted in vivo human
529 whole brain MRI dataset with an ultrahigh isotropic resolution of 250 μm . *Sci Data* **4**,
530 170032.
- 531 54. Weiner KS, Golarai G, Caspers J, Chuapoco MR, Mohlberg H, Zilles K, Amunts K, Grill-
532 Spector K. 2014 The mid-fusiform sulcus: a landmark identifying both cytoarchitectonic and
533 functional divisions of human ventral temporal cortex. *Neuroimage* **84**, 453–465.
- 534 55. Miller JA, D’Esposito M, Weiner KS. 2021 Using Tertiary Sulci to Map the ‘Cognitive Globe’
535 of Prefrontal Cortex. *J. Cogn. Neurosci.* , 1–18.
- 536 56. Yao JK, Voorhies WI, Miller JA, Bunge SA, Weiner KS. 2022 Sulcal depth in prefrontal
537 cortex: a novel predictor of working memory performance. *Cereb. Cortex* , bhac173.
- 538 57. Petrides M. 2019 *Atlas of the Morphology of the Human Cerebral Cortex on the Average*
539 *MNI Brain*. Academic Press.
- 540 58. Petrides M. 2013 *Neuroanatomy of Language Regions of the Human Brain*. Academic
541 Press.
- 542 59. Borne L, Rivière D, Mancip M, Mangin J-F. 2020 Automatic labeling of cortical sulci using
543 patch- or CNN-based segmentation techniques combined with bottom-up geometric
544 constraints. *Med. Image Anal.* **62**, 101651.
- 545 60. Willbrand EH, Ferrer E, Bunge SA, Weiner KS. 2022 Development of human lateral
546 prefrontal sulcal morphology and its relation to reasoning performance. *bioRxiv.* ,
547 2022.09.14.507822. (doi:10.1101/2022.09.14.507822)
- 548 61. Wagenmakers E-J, Farrell S. 2004 AIC model selection using Akaike weights. *Psychon.*
549 *Bull. Rev.* **11**, 192–196.
- 550 62. Burnham KP, Anderson DR. 2004 Multimodel Inference: Understanding AIC and BIC in
551 Model Selection. *Sociol. Methods Res.* **33**, 261–304.
- 552 63. Miller JA, Voorhies WI, Li X, Raghuram I, Palomero-Gallagher N, Zilles K, Sherwood CC,
553 Hopkins WD, Weiner KS. 2020 Sulcal morphology of ventral temporal cortex is shared
554 between humans and other hominoids. *Sci. Rep.* **10**, 17132.
- 555 64. Van Essen DC *et al.* 2012 The Human Connectome Project: a data acquisition perspective.
556 *Neuroimage* **62**, 2222–2231.
- 557 65. Chi JG, Dooling EC, Gilles FH. 1977 Gyral development of the human brain. *Ann. Neurol.*
558 **1**, 86–93.

- 559 66. Armstrong E, Schleicher A, Omran H, Curtis M, Zilles K. 1995 The ontogeny of human
560 gyrification. *Cereb. Cortex* **5**, 56–63.
- 561 67. Allen M, Poggiali D, Whitaker K, Marshall TR, van Langen J, Kievit RA. 2021 Raincloud
562 plots: a multi-platform tool for robust data visualization. *Wellcome Open Res.* **4**, 63.
- 563 68. Fry AF, Hale S. 2000 Relationships among processing speed, working memory, and fluid
564 intelligence in children. *Biol. Psychol.* **54**, 1–34.
- 565 69. Ferrer E, Whitaker KJ, Steele JS, Green CT, Wendelken C, Bunge SA. 2013 White matter
566 maturation supports the development of reasoning ability through its influence on
567 processing speed. *Dev. Sci.* **16**, 941–951.
- 568 70. Kail R, Salthouse TA. 1994 Processing speed as a mental capacity. *Acta Psychol.* **86**,
569 199–225.
- 570 71. Kail RV, Lervåg A, Hulme C. 2016 Longitudinal evidence linking processing speed to the
571 development of reasoning. *Dev. Sci.* **19**, 1067–1074.
- 572 72. Holyoak KJ, Monti MM. 2021 Relational Integration in the Human Brain: A Review and
573 Synthesis. *Journal of Cognitive Neuroscience.* **33**, 341–356. (doi:10.1162/jocn_a_01619)
- 574 73. Welker W. 1990 Why Does Cerebral Cortex Fissure and Fold? In *Cerebral Cortex:
575 Comparative Structure and Evolution of Cerebral Cortex, Part II* (eds EG Jones, A Peters),
576 pp. 3–136. Boston, MA: Springer US.
- 577 74. Amiez C, Sallet J, Hopkins WD, Meguerditchian A, Hadj-Bouziane F, Ben Hamed S, Wilson
578 CRE, Procyk E, Petrides M. 2019 Sulcal organization in the medial frontal cortex provides
579 insights into primate brain evolution. *Nat. Commun.* **10**, 1–14.
- 580 75. Sakai T *et al.* 2012 Fetal brain development in chimpanzees versus humans. *Curr. Biol.* **22**,
581 R791–2.
- 582 76. Krawczyk DC. 2012 The cognition and neuroscience of relational reasoning. *Brain Res.*
583 **1428**, 13–23.
- 584 77. Vendetti MS, Bunge SA. 2014 Evolutionary and developmental changes in the lateral
585 frontoparietal network: a little goes a long way for higher-level cognition. *Neuron* **84**, 906–
586 917.
- 587 78. Aichelburg C, Urbanski M, Thiebaut de Schotten M, Humbert F, Levy R, Volle E. 2016
588 Morphometry of Left Frontal and Temporal Poles Predicts Analogical Reasoning Abilities.
589 *Cereb. Cortex* **26**, 915–932.
- 590 79. Hobeika L, Diard-Detoeuf C, Garcin B, Levy R, Volle E. 2016 General and specialized brain
591 correlates for analogical reasoning: A meta-analysis of functional imaging studies. *Hum.*
592 *Brain Mapp.* **37**, 1953–1969.
- 593 80. Hartogsveld B, Bramson B, Vijayakumar S, van Campen AD, Marques JP, Roelofs K, Toni
594 I, Bekkering H, Mars RB. 2018 Lateral frontal pole and relational processing: Activation
595 patterns and connectivity profile. *Behav. Brain Res.* **355**, 2–11.
- 596 81. Assem M, Glasser MF, Van Essen DC, Duncan J. 2020 A Domain-General Cognitive Core

- 597 Defined in Multimodally Parcellated Human Cortex. *Cereb. Cortex* **30**, 4361–4380.
- 598 82. Kroger JK, Sabb FW, Fales CL, Bookheimer SY, Cohen MS, Holyoak KJ. 2002
599 Recruitment of anterior dorsolateral prefrontal cortex in human reasoning: a parametric
600 study of relational complexity. *Cereb. Cortex* **12**, 477–485.
- 601 83. Crone EA, Wendelken C, van Leijenhorst L, Honomichl RD, Christoff K, Bunge SA. 2009
602 Neurocognitive development of relational reasoning. *Dev. Sci.* **12**, 55–66.
- 603 84. Bunge SA, Helskog EH, Wendelken C. 2009 Left, but not right, rostrolateral prefrontal
604 cortex meets a stringent test of the relational integration hypothesis. *Neuroimage* **46**, 338–
605 342.
- 606 85. Weiner KS. 2019 The Mid-Fusiform Sulcus (sulcus sagittalis gyri fusiformis). *Anat. Rec.*
607 **302**, 1491–1503.
- 608 86. Lopez-Persem A, Verhagen L, Amiez C, Petrides M, Sallet J. 2019 The Human
609 Ventromedial Prefrontal Cortex: Sulcal Morphology and Its Influence on Functional
610 Organization. *J. Neurosci.* **39**, 3627–3639.
- 611 87. Amiez C, Petrides M. 2014 Neuroimaging evidence of the anatomo-functional organization
612 of the human cingulate motor areas. *Cereb. Cortex* **24**, 563–578.
- 613 88. Amiez C, Neveu R, Warrot D, Petrides M, Knoblauch K, Procyk E. 2013 The location of
614 feedback-related activity in the midcingulate cortex is predicted by local morphology. *J.*
615 *Neurosci.* **33**, 2217–2228.
- 616 89. Li Y, Sescousse G, Amiez C, Dreher J-C. 2015 Local morphology predicts functional
617 organization of experienced value signals in the human orbitofrontal cortex. *J. Neurosci.* **35**,
618 1648–1658.
- 619 90. Semendeferi K, Armstrong E, Schleicher A, Zilles K, Van Hoesen GW. 2001 Prefrontal
620 cortex in humans and apes: a comparative study of area 10. *Am. J. Phys. Anthropol.* **114**,
621 224–241.
- 622 91. Reveley C, Seth AK, Pierpaoli C, Silva AC, Yu D, Saunders RC, Leopold DA, Ye FQ. 2015
623 Superficial white matter fiber systems impede detection of long-range cortical connections
624 in diffusion MR tractography. *Proc. Natl. Acad. Sci. U. S. A.* **112**, E2820–8.
- 625 92. Sanides F. 1962 Besprechung. In *Die Architektonik des Menschlichen Stirnhirns: Zugleich*
626 *eine Darstellung der Prinzipien Seiner Gestaltung als Spiegel der Stammesgeschichtlichen*
627 *Differenzierung der Grosshirnrinde* (ed F Sanides), pp. 176–190. Berlin, Heidelberg:
628 Springer Berlin Heidelberg.
- 629 93. Sanides F. 1964 Structure and function of the human frontal lobe. *Neuropsychologia* **2**,
630 209–219.
- 631 94. Wendelken C, Ferrer E, Ghetti S, Bailey SK, Cutting L, Bunge SA. 2017 Frontoparietal
632 Structural Connectivity in Childhood Predicts Development of Functional Connectivity and
633 Reasoning Ability: A Large-Scale Longitudinal Investigation. *J. Neurosci.* **37**, 8549–8558.
- 634 95. Yücel M *et al.* 2002 Paracingulate morphologic differences in males with established
635 schizophrenia: a magnetic resonance imaging morphometric study. *Biol. Psychiatry* **52**, 15–

- 636 23.
- 637 96. Yücel M, Wood SJ, Phillips LJ, Stuart GW, Smith DJ, Yung A, Velakoulis D, McGorry PD,
638 Pantelis C. 2003 Morphology of the anterior cingulate cortex in young men at ultra-high risk
639 of developing a psychotic illness. *Br. J. Psychiatry* **182**, 518–524.
- 640 97. Le Provost J-B *et al.* 2003 Paracingulate sulcus morphology in men with early-onset
641 schizophrenia. *Br. J. Psychiatry* **182**, 228–232.
- 642 98. Fornito A, Malhi GS, Lagopoulos J, Ivanovski B, Wood SJ, Saling MM, Pantelis C, Yücel M.
643 2008 Anatomical abnormalities of the anterior cingulate and paracingulate cortex in patients
644 with bipolar I disorder. *Psychiatry Research: Neuroimaging*. **162**, 123–132.
645 (doi:10.1016/j.pscychresns.2007.06.004)
- 646 99. Fornito A, Yücel M, Wood SJ, Proffitt T, McGorry PD, Velakoulis D, Pantelis C. 2006
647 Morphology of the paracingulate sulcus and executive cognition in schizophrenia.
648 *Schizophr. Res.* **88**, 192–197.
- 649 100. Shim G, Jung WH, Choi J-S, Jung MH, Jang JH, Park J-Y, Choi C-H, Kang D-H, Kwon JS.
650 2009 Reduced cortical folding of the anterior cingulate cortex in obsessive-compulsive
651 disorder. *J. Psychiatry Neurosci.* **34**, 443–449.
- 652 101. Harper L *et al.* 2022 Prenatal Gyrfication Pattern Affects Age at Onset in Frontotemporal
653 Dementia. *Cereb. Cortex* (doi:10.1093/cercor/bhab457)
- 654 102. Meredith SM *et al.* 2012 Anterior cingulate morphology in people at genetic high-risk of
655 schizophrenia. *Eur. Psychiatry* **27**, 377–385.
- 656 103. Gay O, Plaze M, Oppenheim C, Gaillard R, Olié J-P, Krebs M-O, Cachia A. 2017 Cognitive
657 control deficit in patients with first-episode schizophrenia is associated with complex
658 deviations of early brain development. *J. Psychiatry Neurosci.* **42**, 87–94.
- 659 104. Nakamura M, Nestor PG, Shenton ME. 2020 Orbitofrontal Sulcogyral Pattern as a
660 Transdiagnostic Trait Marker of Early Neurodevelopment in the Social Brain. *Clin. EEG*
661 *Neurosci.* **51**, 275–284.
- 662 105. Weickert TW, Goldberg TE, Gold JM, Bigelow LB, Egan MF, Weinberger DR. 2000
663 Cognitive impairments in patients with schizophrenia displaying preserved and
664 compromised intellect. *Arch. Gen. Psychiatry* **57**, 907–913.
- 665 106. Bowie CR, Harvey PD. 2006 Cognitive deficits and functional outcome in schizophrenia.
666 *Neuropsychiatr. Dis. Treat.* **2**, 531–536.
- 667 107. Keefe RSE, Harvey PD. 2012 Cognitive Impairment in Schizophrenia. In *Novel*
668 *Antischizophrenia Treatments* (eds MA Geyer, G Gross), pp. 11–37. Berlin, Heidelberg:
669 Springer Berlin Heidelberg.
- 670 108. Zhang B, Han M, Tan S, De Yang F, Tan Y, Jiang S, Zhang X, Huang X-F. 2017 Gender
671 differences measured by the MATRICS consensus cognitive battery in chronic
672 schizophrenia patients. *Sci. Rep.* **7**, 11821.
- 673 109. Alkan E, Davies G, Evans SL. 2021 Cognitive impairment in schizophrenia: relationships
674 with cortical thickness in fronto-temporal regions, and dissociability from symptom severity.

- 675 *NPJ Schizophr* **7**, 20.
- 676 110. McCutcheon RA, Keefe RSE, McGuire PK. 2023 Cognitive impairment in schizophrenia:
677 aetiology, pathophysiology, and treatment. *Mol. Psychiatry* (doi:10.1038/s41380-023-
678 01949-9)
- 679 111. Kaplan CM, Saha D, Molina JL, Hockeimer WD, Postell EM, Apud JA, Weinberger DR, Tan
680 HY. 2016 Estimating changing contexts in schizophrenia. *Brain* **139**, 2082–2095.
- 681 112. Shinba T, Kariya N, Matsuda S, Arai M, Itokawa M, Hoshi Y. 2022 Near-Infrared Time-
682 Resolved Spectroscopy Shows Anterior Prefrontal Blood Volume Reduction in
683 Schizophrenia but Not in Major Depressive Disorder. *Sensors* **22**.
684 (doi:10.3390/s22041594)
- 685 113. Nazli ŞB, Koçak OM, Kirkici B, Sevindik M, Kokurcan A. 2020 Investigation of the
686 Processing of Noun and Verb Words with fMRI in Patients with Schizophrenia. *Noro*
687 *Psikiyatrs Ars* **57**, 9–14.
- 688 114. Tu P-C, Hsieh J-C, Li C-T, Bai Y-M, Su T-P. 2012 Cortico-striatal disconnection within the
689 cingulo-opercular network in schizophrenia revealed by intrinsic functional connectivity
690 analysis: a resting fMRI study. *Neuroimage* **59**, 238–247.
- 691 115. Pillinger T, Rogdaki M, McCutcheon RA, Hathway P, Egerton A, Howes OD. 2019 Altered
692 glutamatergic response and functional connectivity in treatment resistant schizophrenia: the
693 effect of riluzole and therapeutic implications. *Psychopharmacology* **236**, 1985–1997.
- 694 116. Kang SS, MacDonald AW 3rd, Chafee MV, Im C-H, Bernat EM, Davenport ND, Sponheim
695 SR. 2018 Abnormal cortical neural synchrony during working memory in schizophrenia.
696 *Clin. Neurophysiol.* **129**, 210–221.
- 697 117. Barnes MR *et al.* 2011 Transcription and pathway analysis of the superior temporal cortex
698 and anterior prefrontal cortex in schizophrenia. *J. Neurosci. Res.* **89**, 1218–1227.
- 699
- 700